

Archana Chauhan,[‡] Zeyaul Islam,[‡] Rakesh Kumar Jain* and Subramanian Karthikeyan*

Institute of Microbial Technology (CSIR),
Sector 39-A, Chandigarh 160 036, India

[‡] These authors contributed equally.

Correspondence e-mail: rkj@imtech.res.in,
skarthik@imtech.res.in

Received 21 October 2009

Accepted 9 November 2009

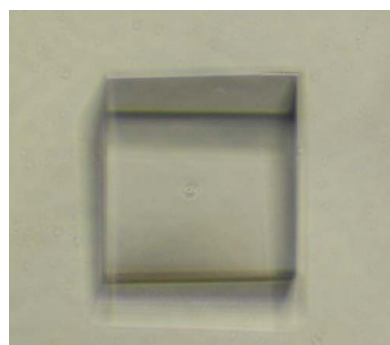
Expression, purification, crystallization and preliminary X-ray analysis of maleylacetate reductase from *Burkholderia* sp. strain SJ98

Maleylacetate reductase (EC 1.3.1.32) is an important enzyme that is involved in the degradation pathway of aromatic compounds and catalyzes the reduction of maleylacetate to 3-oxoadipate. The gene *pnpD* encoding maleylacetate reductase in *Burkholderia* sp. strain SJ98 was cloned, expressed in *Escherichia coli* and purified by affinity chromatography. The enzyme was crystallized in both native and SeMet-derivative forms by the sitting-drop vapour-diffusion method using PEG 3350 as a precipitant at 293 K. The crystals belonged to space group $P2_12_12$, with unit-cell parameters $a = 72.91$, $b = 85.94$, $c = 53.07$ Å. X-ray diffraction data for the native and SeMet-derivative crystal were collected to 2.7 and 2.9 Å resolution, respectively.

1. Introduction

Microbial metabolism of xenobiotics has been recognized as an eco-friendly and cost-effective alternative because of the ability of microbes to undergo rapid genetic evolution (Timmis & Pieper, 1999; Chatterjee & Yuan, 2006; Phale *et al.*, 2007). Degradation of xenobiotic compounds is mediated by a panoply of enzymatic machinery consisting of dehalogenating, dehydrogenating, hydroxylating and hydrolyzing systems (Sariaslani, 1991; Watanabe *et al.*, 2002). The importance of various enzymes in degradation processes has encouraged researchers to carry out detailed studies of these enzymes at the molecular level. This has helped in a greater understanding of the subject with regard to engineering of the catabolic pathways. Maleylacetate (MA) is one of the key intermediates in the degradation of various aromatic compounds, *e.g.* phenol, tyrosine, benzoate, 4-hydroxybenzoate and resorcinol (Gaal & Neujahr, 1979; Shailubhai *et al.*, 1983). Other substrates whose catabolic route contains MA have more complex structures, with unusual substituents such as nitro or sulfo groups and F or Cl atoms *etc.* (Seibert *et al.*, 2004; Perry & Zylstra, 2007). In all of these catabolic pathways MA undergoes aerobic degradation by the enzyme maleylacetate reductase (MaR), a specialized carbon–carbon double-bond reductase. MaR (EC 1.3.1.32) catalyzes the NADH- or NADPH-dependent reduction of MA or substituted MA to 3-oxoadipate (Kaschabek & Reineke, 1992; Seibert *et al.*, 1993; Muller *et al.*, 1996).

MaRs have been purified from variety of microorganisms including Gram-negative bacteria (*Burkholderia cepacia* AC1100, *Ralstonia eutropha* JMP 134 and *Pseudomonas aeruginosa* strain RHO1), Gram-positive bacteria (*Rhodococcus opacus* 1CP, *Neocardia simplex* 3E and *Rhodococcus* sp. strain RHA1) and fungi (*Trichosporon cutaneum* and *Aspergillus niger* strain CBS 513.88/FGSC A1513) (Gaal & Neujahr, 1980; Travkin *et al.*, 1999). Most of the MaRs characterized to date belong to specialized gene clusters that are involved in the degradation of chloroaromatic compounds (Daubaras *et al.*, 1995, 1996; Zaborina *et al.*, 1998; Cai & Xun, 2002). MaRs have also been characterized from pathways that use chlorocatechols as their central intermediates. Multiple sequence alignment of MaRs from different bacterial strains has shown that they share an amino-acid sequence identity of 50–55% with each other. Furthermore,



© 2009 International Union of Crystallography
All rights reserved

database searches revealed that the sequences of the MaRs from most of these strains also have 30–50% identity to the iron-containing type III alcohol dehydrogenases (ADH), a group of enzymes that are able to reduce carbonylic functions or to oxidize alcoholic groups by the use of NADH or NAD, respectively. Many of these MaRs have been characterized extensively in terms of their biochemical, spectroscopic and kinetic properties. In all of these studies, MaR has been reported to be a dimer of about 75–80 kDa consisting of two identical subunits. This is the first report on the structural characterization of a MaR from a nitrophenol-degradation pathway.

MaR was found to be part of the lower pathway of *p*-nitrophenol (PNP) degradation in *Burkholderia* sp. strain SJ98. A gene cluster containing two of the lower pathway PNP-degradation genes (*pnpC* and *pnpD*, encoding benzenetriol dioxygenase and MaR, respectively) was cloned from strain SJ98 and characterized (unpublished results). The 1053 bp *pnpD* encoded a protein of 351 amino acids with a calculated molecular mass of 37 190 Da, which is similar to the monomeric molecular masses of previously purified MaRs. Gel-exclusion chromatography and matrix-assisted laser desorption ionization (MALDI) studies have demonstrated that PnpD is a monomer of about 40 kDa, a property that differs from those of known MaRs (unpublished results). Furthermore, protein-sequence analysis of PnpD using *Basic Local Alignment Search Tool (BLAST)* available at NCBI (<http://www.ncbi.nlm.nih.gov/Blast.cgi>) showed that the protein belongs to the Fe-ADH superfamily, with 78% and 77% sequence identity to MaR from *B. multivorans* strain CDG1 and the iron-containing alcohol dehydrogenase from *B. multivorans* ATCC 17616, respectively. Thus, theoretically there is an equal probability of PnpD being either a MaR or an ADH. However, functional studies involving biochemical, spectroscopic and kinetic characterization of the purified PnpD showed that this protein acts on MA, thus showing MaR activity, but does not act on the usual substrates of ADHs. Hence, it can be concluded that PnpD is a functional MaR. A detailed protein-sequence analysis revealed that this protein contains four cysteine residues at positions Cys88, Cys219, Cys226 and Cys242. Also, inhibition studies have shown that thiol-blocking reagents such as *p*-chloromercuribenzoate and Hg²⁺ inhibit the activity of this protein, indicating the importance of the cysteine residues in its catalytic activity. This observation is in agreement with previous studies, which have indicated the role of highly conserved cysteine residues, *i.e.* Cys242 at the C-terminus, in the catalytic activity of MaR (Gaal & Neujahr, 1980; Kaschabek & Reineke, 1993). Furthermore, we also found an NAD-binding sequence motif in the N-terminus of PnpD (Wierenga *et al.*, 1986). These observations therefore suggest that PnpD from *Burkholderia* sp. strain SJ98 consists of two domains: an N-terminal NAD-binding domain and a C-terminal active-site domain.

To date, only one MaR structure is available from *Agrobacterium tumefaciens* (strain C58; PDB code 3hl0; C. Chang, E. Evdokimova, A. Mursleen, A. Savchenko, A. Edwards & A. Joachimiak, unpublished work). A preliminary X-ray analysis of MaR from *Rhizobium* sp. strain MTP-10005 has also been reported (Fujii *et al.*, 2008). Three-dimensional structure determination of PnpD may help in understanding its specific substrate recognition of MA and not of the substrate of type III alcohol dehydrogenases despite its high (77%) sequence identity with the latter. Additionally, analysis of the crystal structure of PnpD could shed light on the residues that participate in the catalytic conversion of MA to 3-oxoadipate in the PNP-degradation pathway of *Burkholderia* sp. strain SJ98. In this paper, we report the detailed procedure of purification and successful crystallization of PnpD from *Burkholderia* sp. strain SJ98 as well as preliminary X-ray characterization of these crystals.

2. Material and methods

2.1. Cloning

A pair of oligonucleotides (forward, ExpMaR_F, 5'-ACTTCAT-ATGCAATCGTCGTTA-3', with *Nde*I restriction site shown in bold; reverse, ExpMaR_R, 5'-CTTCAAGCTTTCATGGTCGTC-CT-3', with *Hind*III restriction site shown in bold) was synthesized to amplify the *pnpD* gene from the genomic DNA of *Burkholderia* sp. strain SJ98 by the polymerase chain reaction (PCR). The PCR-amplified DNA was digested with restriction endonucleases *Nde*I and *Hind*III and ligated into the protein-expression vector pET28c(+) at the *Nde*I and *Hind*III sites. The resulting plasmid pET28c(+)-PnpD was checked for insertion of the *pnpD* gene by DNA sequencing. The recombinant plasmid pET28c(+)-PnpD DNA was transformed into *Escherichia coli* BL21 (DE3) cells for the expression of N-terminally His-tagged protein.

2.2. Protein expression and purification

2.2.1. Native PnpD. Seed cultures that were grown overnight in Luria broth (LB) containing 25 mg ml⁻¹ kanamycin were used as an inoculum for growing large-scale cultures in Terrific broth medium (12 g Bacto tryptone, 24 g Bacto yeast extract, 4.0 ml glycerol, 2.3 g KH₂PO₄, 12.5 g K₂HPO₄, 1000 ml distilled water pH 7.0) containing 25 mg ml⁻¹ kanamycin at 298 K. The cells were grown until the absorbance at 600 nm reached a value of between 1 and 1.5. Expression of the *pnpD* gene was induced by adding isopropyl β -D-1-thiogalactopyranoside (IPTG) to a final concentration of 0.1 mM and the temperature was reduced to 291 K. After half an hour of induction, the cells were harvested by centrifugation at 3500g for 15 min at 277 K and washed with 10 mM phosphate buffer pH 7.3. Cells were resuspended in lysis buffer (50 mM sodium phosphate buffer pH 8.0, 300 mM NaCl, 10 mM imidazole) containing protease inhibitors (1 mM phenylmethylsulfonyl fluoride, 1 μ g ml⁻¹ pepstatin and 1 μ g ml⁻¹ leupeptin) and lysed by sonication (Sonics, 10–30 s bursts at 70% power). Cell debris was pelleted by centrifugation at 8000g and 277 K for 30 min. The supernatant was loaded onto an Ni-NTA (Qiagen, Germany) column previously equilibrated with lysis buffer. The unbound proteins were washed with wash buffer (50 mM sodium phosphate buffer pH 8.0, 300 mM sodium chloride, 50 mM imidazole) and the bound protein was eluted using elution buffer (50 mM sodium phosphate buffer pH 8.0, 300 mM sodium chloride, 250 mM imidazole). The fractions containing the enzyme were pooled and dialyzed overnight against a buffer consisting of 20 mM Tris-HCl pH 8.0, 20 mM NaCl. The protein was concentrated by centrifugation at 2000g at 277 K using an Amicon 10 kDa molecular-weight cutoff concentrator (Millipore, USA). The protein was analyzed by size-exclusion chromatography using a 120 ml Superdex 200 column (GE Healthcare, USA) equilibrated with 10 mM Tris-HCl pH 8.0, 50 mM NaCl with a load volume of 1 ml. The purity of the protein was checked by SDS-PAGE analysis.

2.2.2. Selenomethionine-labelled PnpD. Sequence analysis of PnpD showed the presence of ten methionine residues and a molecular weight of 40 kDa, making it a good candidate for phasing by selenomethionine labelling. Selenomethionine-labelled protein was prepared using methionine-biosynthesis inhibition (Bottomley *et al.*, 1994). A 10 ml LB culture containing 25 mg ml⁻¹ kanamycin was grown overnight at 310 K and gently pelleted by centrifugation at 2000g and 277 K for 5 min. This pellet was resuspended in 10 ml M9 minimal medium and used to inoculate selenomethionine growth medium comprising M9 minimum medium plus sterile-filtered MgSO₄ (1 mM), glucose [0.4% (w/v)], thiamine [0.00005% (w/v)] and

Table 1

Data-collection statistics for PnpD.

Values in parentheses are for the highest resolution shell.

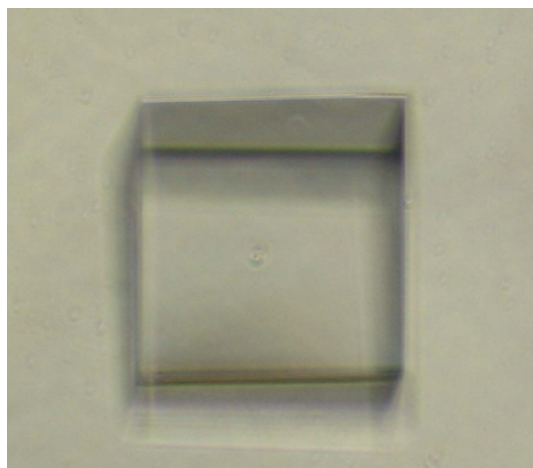
	Native	SeMet		
		Peak	Inflection	Remote
Wavelength (Å)	1.542	0.9786	0.9788	0.9747
Space group	$P2_12_12$	$P2_12_12$	$P2_12_12$	$P2_12_12$
Unit-cell parameters (Å)				
<i>a</i>	72.91	72.65	72.63	72.65
<i>b</i>	85.94	86.15	86.10	86.17
<i>c</i>	53.07	53.43	53.40	53.45
Resolution range (Å)	50.0–2.70 (2.80–2.70)	50.0–2.90 (3.00–2.90)	50.0–2.90 (3.00–2.90)	50.0–2.90 (3.00–2.90)
Completeness (%)	97.5 (81.9)	96.0 (70.7)	95.9 (68.3)	96.0 (69.6)
$R_{\text{merge}}^{\dagger} (%)$	8.4 (29.0)	9.9 (28.2)	10.3 (28.5)	9.9 (27.3)
Mean $I/\sigma(I)$	19.8 (3.2)	22.77 (3.5)	20.02 (3.4)	21.85 (3.6)
No. of observed reflections	55891	57340	56607	56965
No. of unique reflections	9460	7553	7553	7589
Redundancy	5.9 (3.3)	7.6 (3.3)	7.5 (3.3)	7.5 (3.1)
No. of molecules per ASU	1			
Solvent content (%)	42			

† $R_{\text{merge}} = \sum_{hkl} \sum_i |I_i(hkl) - \langle I(hkl) \rangle| / \sum_{hkl} \sum_i I_i(hkl)$, where $I(hkl)$ is the intensity of reflection hkl , \sum_{hkl} is the sum over all reflections and \sum_i is the sum over i measurements of reflection hkl .

FeSO_4 (15 mM). Cells were grown at 310 K to an OD_{600} of 0.3, at which point L-selenomethionine (Sigma; 50 mg l⁻¹), L-leucine (50 mg l⁻¹), L-lysine (100 mg l⁻¹), L-isoleucine (50 mg l⁻¹), L-phenylalanine (100 mg l⁻¹), L-threonine (100 mg l⁻¹) and L-valine (50 mg l⁻¹) were added, followed by the addition of 0.1 mM IPTG after 15 min. Cells were grown to an OD_{600} of 1.0 at 291 K and were then harvested by centrifugation at 3500 g and 277 K for 15 min. Purification of selenomethionine-labelled PnpD was carried out in an identical manner to that of native protein and the incorporation of selenomethionine was verified by MALDI-TOF mass spectroscopy.

2.3. Crystallization

PnpD protein at a concentration of 15 mg ml⁻¹ in 20 mM Tris pH 8.0 and 20 mM NaCl buffer was used for crystallization experiments. Prior to crystallization, the protein was mixed with 5 mM NADH and incubated on ice for 30 min. Initial crystallization screens were set up using PEG/Ion Screen (Hampton Research, USA) and the sitting-drop vapour-diffusion method in 96-well crystallization plates (MRC Laboratory) at 293 K. Drops containing 1 μ l protein solution and 1 μ l

**Figure 1**

Single crystal of PnpD. The overall dimensions of the typical crystal are 300 \times 300 \times 200 μ m.

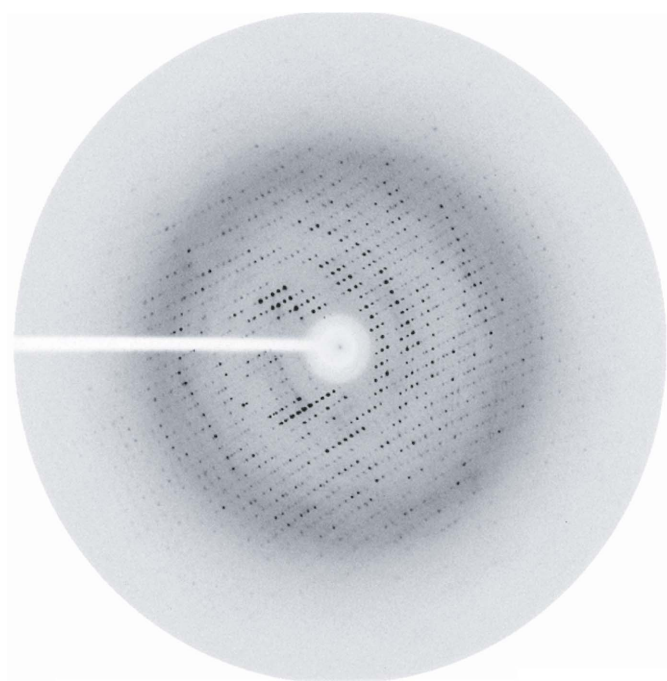
reservoir solution were equilibrated against 60 μ l reservoir solution. Potential crystallization conditions from the screen were optimized using the sitting-drop vapour-diffusion method in 24-well crystallization plates (CombiClover Jr, Emerald BioSystems) at 293 K. Drops containing 2 μ l protein solution and 2 μ l reservoir solution were equilibrated against 200 μ l reservoir solution. Crystals of selenomethionine-labelled protein were obtained using the same conditions as used for the native protein.

2.4. Data collection and analysis

A single crystal of native protein was soaked in a cryoprotectant solution composed of mother liquor plus 15% (v/v) glycerol for 45 s and flash-cooled in a nitrogen stream at 100 K. Diffraction data were collected using a MAR345 image-plate detector (MAR Research, Germany) and a Rigaku rotating-anode generator (UltraX 18) generating $\text{Cu K}\alpha$ radiation operated at 50 kV and 90 mA and equipped with Osmic confocal Max-Flux optics. The crystal-to-detector distance was fixed at 200 mm. A complete data set was collected using 180 frames of 1° oscillation with an exposure time of 5 min per image. For SeMet crystals, diffraction data were collected on the ESRF BM14 beamline (European Synchrotron Radiation Facility, Grenoble, France) using a MAR Mosaic CCD detector (225 mm) at three different wavelengths (peak, inflection and remote absorption edge for Se). For each wavelength, 360 frames of 1° oscillation were collected with an exposure time of 20 s per frame. All the images were indexed, integrated and scaled using the HKL-2000 suite of programs (Otwinowski & Minor, 1997).

3. Results and discussion

The gene *pnpD* encoding PnpD was amplified by PCR from the genomic DNA of *Burkholderia* sp. strain SJ98. DNA sequencing confirmed that the PCR product contained 1053 bp and shared 78% identity with the *MaR* from *B. multivorans* strain CDG1. The *pnpD*

**Figure 2**

Diffraction pattern of a PnpD crystal collected at the in-house X-ray facility. The crystal diffracted to 2.7 Å resolution.

gene was then cloned into the expression vector pET28c(+) and recombinant N-terminally His₆-tagged PnpD was overexpressed in *E. coli* BL21 (DE3) cells. The protein was purified to homogeneity by Ni-NTA affinity chromatography, concentrated to 15 mg ml⁻¹ (in 20 mM Tris-HCl pH 8.0, 10 mM NaCl) and immediately used for crystallization. To obtain good-quality crystals, it was necessary to incubate the protein with 5 mM NADH for 30 min on ice just prior to crystallization. Diffracting crystals (Fig. 1) were obtained after 3–4 d at 293 K using 0.2 M ammonium phosphate dibasic and 20% (w/v) polyethylene glycol 3350 (PEG 3350) as precipitant. The crystal belonged to the orthorhombic space group *P*2₁2₁2, with unit-cell parameters *a* = 72.91, *b* = 85.94, *c* = 53.07 Å, and diffraction data (Fig. 2) were collected to 2.7 Å resolution. SeMet-labelled protein crystals were obtained using the same condition as used for the native protein and data were collected to 2.9 Å resolution using synchrotron radiation on the ESRF BM14 beamline. Data-collection statistics are shown in Table 1. Assuming the presence of one molecule per asymmetric unit with a molecular mass of 39 183 Da as determined by MALDI, the calculated Matthews value (*V*_M) was 2.2 Å³ Da⁻¹, which is within the range expected for protein crystals (Matthews, 1968). Further structure determination using the MAD/SAD method is in progress.

We would like to thank Dr Hassan Belhrali for his help during data collection at ESRF, France and Dr Purnananda Guptasarma for his help in carrying out the MALDI analysis. We acknowledge the research fellowships awarded by the Council of Scientific and Industrial Research (CSIR), Government of India. We also thank Department of Biotechnology (DBT), Government of India and the National Institute of Immunology (NII), New Delhi for the financial assistance provided for the data collection in France.

References

Bottomley, M. J., Robinson, R. C., Driscoll, P. C., Harlos, K., Stuart, D. I., Aplin, R. T., Clements, J. M., Jones, E. Y. & Dudgeon, T. J. (1994). *J. Mol. Biol.* **244**, 464–468.

Cai, M. & Xun, L. (2002). *J. Bacteriol.* **184**, 4672–4680.

Chatterjee, R. & Yuan, L. (2006). *Trends Biotechnol.* **24**, 28–38.

Daubaras, D. L., Danganan, C. E., Hubner, A., Ye, R. W., Hendrickson, W. & Chakrabarty, A. M. (1996). *Gene*, **179**, 1–8.

Daubaras, D. L., Hershberger, C. D., Kitano, K. & Chakrabarty, A. M. (1995). *Appl. Environ. Microbiol.* **61**, 1279–1289.

Fuji, T., Goda, Y., Yoshida, M., Oikawa, T. & Hata, Y. (2008). *Acta Cryst. F* **64**, 737–739.

Gaal, A. & Neujahr, H. Y. (1979). *J. Bacteriol.* **137**, 13–21.

Gaal, A. B. & Neujahr, H. Y. (1980). *Biochem. J.* **185**, 783–786.

Kaschabek, S. R. & Reineke, W. (1992). *Arch. Microbiol.* **158**, 412–417.

Kaschabek, S. R. & Reineke, W. (1993). *J. Bacteriol.* **175**, 6075–6081.

Matthews, B. W. (1968). *J. Mol. Biol.* **33**, 491–497.

Muller, D., Schlamann, M. & Reineke, W. (1996). *J. Bacteriol.* **178**, 298–300.

Otwinowski, Z. & Minor, W. (1997). *Methods Enzymol.* **276**, 307–326.

Perry, L. L. & Zylstra, G. J. (2007). *J. Bacteriol.* **189**, 7563–7572.

Phale, P. S., Basu, A., Majhi, P. D., Deveryshtey, J., Vamsee-Krishna, C. & Shrivastava, R. (2007). *OMICs*, **11**, 252–279.

Sariaslani, F. S. (1991). *Adv. Appl. Microbiol.* **36**, 133–178.

Seibert, V., Stadler-Fritzsche, K. & Schlamann, M. (1993). *J. Bacteriol.* **175**, 6745–6754.

Seibert, V., Thiel, M., Hinner, I. S. & Schlamann, M. (2004). *Microbiology*, **150**, 463–472.

Shailubhai, K., Somayaji, R., Rao, N. N. & Modi, V. V. (1983). *Experientia*, **39**, 70–72.

Timmis, K. N. & Pieper, D. H. (1999). *Trends Biotechnol.* **17**, 200–204.

Travkin, V. M., Linko, E. V. & Golovleva, L. A. (1999). *Biochemistry (Mosc.)*, **64**, 625–630.

Watanabe, K., Futamata, H. & Harayama, S. (2002). *Antonie Van Leeuwenhoek*, **81**, 655–663.

Wierenga, R. K., Terpstra, P. & Hol, W. G. (1986). *J. Mol. Biol.* **187**, 101–107.

Zaborina, O., Daubaras, D. L., Zago, A., Xun, L., Saido, K., Klem, T., Nikolic, D. & Chakrabarty, A. M. (1998). *J. Bacteriol.* **180**, 4667–4675.